Asian Journal of Chemistry Vol. 18, No. 3 (2006), 1919–1934

Chemical and Structural Properties of Titanium Dioxide Modified Jordanian Zeolitic Tuffs and Their Potential for the Removal of Phenolics in Aqueous Media

NASSER M. NASSER, SALEM M. MUSLEH* and GHAZI DERWISH
Chemistry Departement, University of Jordan, 19142, Amman, Jordan
E-mail: sumusleh@lycos.com

Titanium dioxide was deposited on the native Jordanian zeolitic tuff. XRF, XRD, SEM and FTIR techniques were used to characterize the chemical and structural properties of modified and unmodified samples. The zeolitic tuff supported titanium oxide was used in preliminary experiments to study their interaction with aqueous phenol solution under thermal and photochemical conditions, in the presence and absence of hydrogen peroxide. The results showed that titanium oxide has interacted with zeolitic tuff and caused some structural changes. These were reflected in the surface area of the samples and their activity in the phenol reactions.

Key words: Zeolitic tuff, Adsorption, Phenols, Modification, Titanium oxide.

INTRODUCTION

Zeolitic tuff deposits, rich in Phillipsite, were first discovered in Jordan in 1987 in the eastern part of the country at Jebal Aritain[1]; since then zeolites have also been found in other localities, mainly in the basaltic areas in the northeastern region of Jordan[2, 3]. The chemical and physical properties of the Aritain zeolites are similar to those found in Italy. However, their ammonium exchange and moisture adsorption capacities are found to be higher than those of the Italian zeolites[2]. Besides phillipsite other species were found in these deposits, they are mainly faujasite and chabazite. It is interesting to note the presence of relatively rare faujasite in Jordanian tuff formations[4]. The unique combination of physical and chemical properties of zeolites makes them suitable for a wide range of applications in industry, agriculture, medicine and environment[5–8].

The present work plans to try and impart some useful properties on the local materials with the object of widening their applications to include their possible use in the removal of pollutants from an aqueous media.

Towards this end zeolitic tuffs from Jebal Aritain are selected because of their known zeolitic contents[1]. The inhomogeneity of the zeolitic tuff is emphasized by the predominance of the phillipsite with its rather narrow pore size, along site and chabazite with their greater ability to accept molecules, such as organic phenolic pollutants, into their structure.

*Basic Science Department, Prince Abdaullah Bin Ghazi Faculty of Science and Information Technology, Al-Balqa Applied University, Al-Salt, 19117, Jordan.

Phenols, particularly chlorophenols, whether from the chlorination of water or from industrial and agricultural sources, are serious pollutants of water and soils[9, 10]. It has been reported that "concentration of phenols in unpolluted waters is usually less than 0.02 mg L^{-1}".[11] However, the WHO's "Guidelines for drinking water quality" gives the level of phenols for drinking water[12] as 0.001 mg L^{-1}.

Chlorinated compounds in the soil and in water sources have been found in some areas of Jordan[13]. One serious possible source for that is the excessive use of chlorinated pesticides in Jordan valley[14].

It was therefore decided to investigate the possible modification of Jordanian zeolitic tuff by titanium oxide to improve their surface properties that could enhance their use as agents for removal of phenolics from aqueous solution using both thermal and photolytic reactions with and without the presence of hydrogen peroxide. The preparation and characterization of these modified tuffs are reported in this paper together with the preliminary results of their possible use for the removal of phenol from aqueous solution.

EXPERIMENTAL

Preparation of starting materials

Raw zeolitic tuff samples (Z) from Jebal Aritain in Jordan were kindly donated by the Natural Resources Authority (NRA), Jordan. The zeolitic tuff rock was crushed gently by hammer and hand ground by a glass rod. The ground material was sieved at different meshes, and the portion with particle size 500–1000 μm was selected for the purpose of this investigation.

The sample was passed through a magnetic separator (high dry magnetic separator model MIH-13) at NRA, which gave two samples: one with high iron content (MZ) and the other with low iron content (NZ). The sample with low iron content was divided into three portions; the first was left unwashed (NZ), the second was subjected to brine water washing (BZ) and the third was washed with distilled water (DWZ). To ensure their zeolitic contents the samples were characterized by their powder XRD patterns.

Washing with brine: 100 g sample was treated with 2 M NaCl solution (250 mL) with stirring for 1 h at 500 rev/min. It was allowed to settle and supernatant was washed with distilled water several times until no chloride ions were deleted in the eluted water, by using $AgNO_3$ solution.

Washing with distilled water: A sample of 100 g was washed three times with distilled water using mechanical stirrer 500 rev/min for 1 h.

All the samples, the magnetic and the nonmagnetic, the washed and the unwashed were dried in an oven overnight at 105°C and were kept in a desiccator over anhydrous $CaCl_2$.

Preparation of Titanium Dioxide: Titanium dioxide was prepared by means of $TiCl_4$ hydrolysis at room temperature; 10 mL of it was added gradually to 400 mL of distilled water. The mixture was subsequently neutralized with 50 mL 25% ammonia solution and stirred for 2 h, filtered, dried at 100°C and kept at 250°C in muffle furnace for 16 h and then kept desiccated over anhydrous $CaCl_2$.

Modification of Zeolitic Tuff samples with Titanium Dioxide (TiO_2)

A 10 g portion of the prepared tuff samples was stirred with distilled water

(400 mL) for 5 min. Then 10 mL of $TiCl_4$ (0.091 mol) was added gradually to the mixture at room temperature. The mixture was subsequently neutralized with 50 mL 25% ammonia solution and stirred for 2 h, filtered, dried at 100°C and kept at 250°C in a muffle furnace for 16 h. The above procedure gave the TiO_2 loaded samples TZ, TMZ, TNZ, TDWZ and TBZ.

Characterization of Zeolitic Samples

All samples were characterized by ascertaining their chemical composition, mineral constitution and chemical characterization, as well as their surface morphology and adsorption capacity.

The chemical composition was determined by XRF technique at JNRA. The instrument used was Diano-2023. The operating conditions were followed as presented by the manufacturer. Thus, 0.8 g of the sample was thoroughly mixed with 7.2 g of lithium tetraborate ($Li_2B_4O_7$) in a platinum crucible, which was introduced into an automatic fluxer (Leco Corp. model FX-200) where a temperature program was affected starting from room temperature to 1200°C. The melt was then poured into a casting dish and allowed to cool. The resultant glassy disk was used for XRF analysis. The mineral constitution of the samples was determined at JNRA by powder XRD technique, using X'pert instrument fitted with a Phillips X-ray tube giving CoK_α radiation at $\lambda = 1.77892$ Å, at 40 kV and 40 Ma. The chemical characterization of the samples was investigated by FTIR spectrometry using a KBr matrix. The instrument used was a Jasco FTIR-410 spectrophotometer, of scanning range between 4000–400 cm^{-1}. The surface morphology of the samples was studied using scanning electron microscope (SEM) type XL-30 W/TMP/2000 at 20 kV. All samples were carbon plated.

Surface Area Estimation

The surface areas for samples were estimated using the methylene blue (MB) method[15]. Methylene blue adsorption can be used for the measurement of surface areas of clay minerals[16, 17]. The method has advantage over BET gas adsorption measurements in being readily applicable to a wide range of areas and especially to minerals under aqueous conditions. The method is simple, rapid and economical[18]. Weight samples of adsorbent in the range 15–105 mg were placed separately in 250 mL stoppered Erlenmeyer flasks and 100 mL of 50 ppm methylene blue solution was added to each. To achieve equilibrium for the adsorption of dyes by clay minerals an incubation period of 12–24 days has been reported[19]. In the present study the mixtures, together with a control sample of MB, were left in subdued light at room temperature for a long period of six weeks to be sure that equilibrium is reached. Spectrophotometer analysis of adsorbate solution was carried out with a Milton Roy-Spectronic-1201 in 10 mm silica sample cells, using the calibration Beer law plot at $\lambda = 612$ nm.

Reactions of Aqueous Phenol

Reactions of aqueous phenol in the presence of the modified and unmodified zeolitic tuff samples were carried out both thermally and photochemically as follows:

Thermal reaction of aqueous phenol in the presence of hydrogen peroxide: In these reactions, the reaction mixture contained 5000 ppm phenol, to which was added H_2O_2 (33% v/v), so the total volume of mixture was 150 mL containing 1/65% (v/v) H_2O_2. When preparing the standard stock solution, care was taken to ensure that complete dissolution of phenol had occurred. The reaction flask was held in an oil bath at a temperature of 20±2°C, which allowed easy follow-up of the reaction with time. The reaction mixture was continuously stirred at moderate speed. Portions of 0.2 mL each were drawn at certain time intervals and transferred into sample bottles (25 mL) fitted with screw caps. A 0.25 mL sodium sulfite solution (0.5 m) was immediately added to completely reduce the remaining H_2O_2 and terminate the reaction.

For thermal catalytic reactions 0.15 g was taken from the prepared catalyst sample and introduced into the reaction vessel and the same procedure was followed.

Photochemical reaction of aqueous phenol with hydrogen peroxide: In reaction mixture containing (5000) ppm phenol, to which (33% v/v) H_2O_2 was added. So the total volume mixture is (150 mL) contained (0.22% v/v) H_2O_2. The reaction mixture was continuously stirred at moderate speed. Portions of 0.2 mL of the mixture were withdrawn at certain time intervals and transferred into sample bottles (25 mL) fitted with screw caps. Sodium sulfite solution was immediately added (0.2 mL, 0.5 M) prior to analysis.

For photocatalytic reaction the above procedure was repeated with addition of 0.15 g of each of the prepared catalyst samples.

Analysis of Phenol

The procedure followed for the spectrophotometric determination of phenol in aqueous solution was according to that described by Blo *et al.*[20]. Samples were derivatives after successive additions of the following reagents: 0.5 mL 4-amino antipyrine (4-Aap), 2% 2 mL KCl (0.05 m), 1 mL $AgNO_3$ (0.08 M), 2 mL borax (pH 9) and 1 mL dextrin (0.6% w/v). The volume of the mixture was increased by distilled water to 25 mL in the screwed sample bottles, which were placed in water batch at 41 ± 2°C for 45 min before analysis.

After derivatization, the sample bottles were allowed to cool, and then the content of each was transferred to a separatory funnel containing 75 mL distilled water. About 12 mL $CHCl_3$ were then added and separated in separatory funnel.

The chloroform extract was collected in a 25 mL flask and the volume was completed to the mark. A 2.0 mL portion was withdrawn by pipette and placed in a 10 mL screwed cylindrical glass tube, diluted by adding 6 mL $CHCl_3$. For photochemical reaction in aqueous phenol, because of lower concentration of phenol used, the separation of the derivatized phenol was extracted by 5 mL of $CHCl_3$, before spectrophotometric concentration measurements.

The phenol concentration of the final solution was determined using spectrophotometric measurement at 455 nm. To obtain calibration curve for phenol, the following standard solutions in H_2O were prepared: 4, 8, 12, 16 and 20 ppm; these standards were then subjected to the above analytic derivatization procedure before spectrophotometric measurement were carried out.

RESULTS AND DISCUSSION

Characterization of titanium dioxide samples

XRD pattern of the prepared TiO_2 sample is found to be identical with peaks of anatase given in the XRD card No 21-1272 of Joint Committee on Powder Diffraction standard (JCPDS), as shown in Table-1.

TABLE-1
POWDER XRD PEAKS FOR TiO_2

TiO_2 sample		JCPDS (card no. 21-1272)	
2θ	I/I*	2θ	I/I*
29.45	100	29.44	100
44.37	39	44.20	20
56.31	31	56.43	35
63.87	24	63.50	20

*Normalized values.

The FTIR results showed two broad peaks, one about 467 cm^{-1} while the other weaker at about 689 cm^{-1} and the weak shoulder at 793 cm^{-1}. These agree with the reported values of anatase TiO_2 peaks, which are: strong band between 525–460, broadband at 700 cm^{-1} and the shoulder at 790 cm^{-1}.[15]

Chemical composition of zeolitic samples

All zeolitic samples were analyzed by XRF to determine their chemical composition; the results are given in Table-2. The difference from 100% is loss on ignition.

The indicator ratios for zeolitic samples, *i.e.*, SiO_2/Al_2O_3 and (Mg + Ca + Na + K) oxides/Al_2O_3 are given in Table-3. The resulting oxides are typically > 2 for the former and 1 for the latter. These indicator ratios fall in the right range for typical zeolites, thus showing the zeolitic nature of the tuff samples.

TABLE-2
CHEMICAL COMPOSITION OF MODIFIED AND UNMODIFIED ZEOLITIC SAMPLES

Oxide (%)	Z	TZ	MZ	TMZ	NZ	TNZ	DWZ	TDWZ	BZ	TBZ
Fe_2O_3	12.19	10.82	15.71	13.53	2.54	2.08	1.46	1.50	2.03	1.24
MnO	0.14	0.00	0.23	0.00	0.00	0.00	0.00	0.00	0.00	0.00
TiO_2	3.30	35.75	3.44	39.04	0.97	35.89	0.80	35.90	0.95	41.18
CaO	7.06	0.00	5.56	0.00	10.95	0.00	9.17	0.00	12.28	0.00
K_2O	1.03	0.16	0.75	0.05	3.10	0.65	2.36	0.66	2.93	0.61
P_2O_5	0.22	0.00	0.24	0.01	0.21	0.00	0.18	0.00	0.25	0.00
SiO_2	35.78	23.86	34.70	21.48	40.56	25.37	56.44	24.13	41.15	21.00
Al_2O_3	10.04	0.47	9.12	0.01	14.25	0.54	10.45	0.45	14.13	0.00
MgO	9.81	6.86	11.30	7.10	2.97	1.69	2.29	1.75	3.16	1.41
Na_2O	1.95	0.00	1.49	0.00	1.82	0.00	3.33	0.00	2.74	0.00
L.O.I	18.21	22.08	17.46	18.79	22.36	33.78	13.52	35.61	20.02	34.56

TABLE-3
INDICATOR RATIOS FOR ZEOLITIC SAMPLES

Sample	SiO_2/Al_2O_3	(Mg + Ca + Na + K) oxides/Al_2O_3
Z	3.56	2.00
MZ	3.80	2.09
NZ	2.85	1.32
DWZ	5.40	1.64
BZ	2.88	1.48

The brine washed zeolitic BZ sample shows the highest Na^+ and K^+ content as shown in Table-4. It shows the highest cation content, not only because it was washed with brine, but also because the high percentage of alumina relative to silica requires more monovalent or divalent cations to rectify the overall charge and to minimize the free energy of the sample as shown in Table-5.

TABLE-4
CATION CONTENT IN THE UNMODIFIED ZEOLITIC SAMPLES

Sample	$(K_2O + Na_2O)/(Al_2O_3 + SiO_2)$%
Z	7.1
MZ	5.1
NZ	8.9
DWZ	8.5
BZ	10.2

TABLE-5
Al_2O_3, Fe_2O_3 AND TiO_2 RELATIVE TO SiO_2
IN THE UNMODIFIED SAMPLES

Sample	Al_2O_3/SiO_2	Fe_2O_3/SiO_2	TiO_2/SiO_2
Z	28.0	34.1	9.2
MZ	26.0	45.2	9.9
NZ	35.1	6.3	2.3
DWZ	18.5	2.6	1.4
BZ	34.8	4.9	2.3

It is clear that MZ sample contains the highest iron and titanium content of all samples.

Effect of loading of titanium dioxide on zeolitic tuffs

From the chemical composition shown in Table-2, it is clear that the silica content has decreased markedly. This may be due to the production of HCl during the metal oxide deposition on the sample. Ammonia is added to neutralize the acid and control the reaction.

The contents of Ca, K and Na have been drastically decreased in the modified samples because such metals react easily with the produced hydrochloric acid to

give the corresponding soluble chlorides, exceptions being with Mg and Fe, showing marked decrease, but more than others.

All samples of modified zeolite were subjected to calcination at 250°C, to increase the surface acidity through the removal of structural hydroxyl groups, (Bronsted acid sites) in pairwise fashion, giving rise to three-coordinated alumina with loss of water.

It is clear that there is decease in alumina content in all the modified zeolitic samples. This may be due to the replacement of alumina in the zeolitic samples by titanium, which is in agreement with previous observations[17].

Surface morphology

The surface morphology for Jordanian zeolitic tuffs studied agrees with the results obtained in previous studies[18]. It shows clearly the phillipsite crystals as the predominant mineral in the samples.

For the loaded titanium oxide samples they indicate the presence of cavities, channels and kinks due to the void nature of the zeolitic tuff surfaces. These figure the loading of titanium as white spheres on the surface of the zeolitic samples.

Mineral constitution of zeolitic samples

The mineral constitutions of the zeolitic samples are shown in Table-6. It is clear that for all unmodified samples, the phillipisite is the predominant mineral, with faguasite, calcite and anorthite as minor constituents, while chabasite and forsterite are present in trace amounts.

Hematite was found to be in trace amount. These results are in agreement with other research done on the Jordanian zeolite[19].

TABLE-6
MINERAL CONTENTS OF MODIFIED AND UNMODIFIED ZEOLITIC TUFF SAMPLES

Mineral	Z	TZ	MZ	TMZ	NZ	TNZ	DWZ	TDWZ	BZ	TBZ
Phillipsite	***	**	***	*	***	***	***	***	***	***
Faujasite	**	*	**	*	*	**	**	*	**	*
Chabsite	*	–	*	–	*	–	*	–	*	–
Calcite	**	–	**	–	**	–	**	–	**	–
Forsterite	*	–	*	–	*	–	*	–	*	–
Anorthite	**	*	**	*	**	*	**	**	**	**
Hematite	*	–	*	*	–	–	–	–	–	–
Anatase	–	***	–	***	–	***	–	***	–	***

***major; **minor; *trace

It is noticed that anatase titanium oxide has become dominant in all the modified samples. It is clear that the minerals that seemed to be minor in the unmodified samples become trace after modification with titanium oxide and those that seemed to be trace have completely disappeared.

This is in agreement with what was expected, since titanium dioxide loading

process has made it the predominant component in the modified samples. Samples that used to contain high percentage of iron (Z and MZ) have shown good loading of titanium oxide on their surfaces when modified. Other samples of titanium oxide have significant influence on the presence of Phillipsite that remain major constituents in the modified samples TNZ and TDWZ.

Samples loaded with TiO_2 have been subjected to a thermal treatment through calcination process at 250°C. This does not affect the appearance of zeolite and other minerals. Thermal treatment has shown not to affect the mineral constitutions unless the temperature is raised to 750°C and above[21].

Chemical constitution of zeolitic samples

The spectra of the zeolitic framework aluminosilicate lie in three regions; the strongest bands appear in the 1200–950 cm^{-1} region, and these can be characterized as due to asymmetric Si—O—Si(Al) stretching vibrations. The second region of medium intensity absorption lies in the 850–550 cm^{-1} region that can be characterized as due mainly to the symmetric stretching vibrations. The third region of strong intensity absorption usually lies between 500–400 cm^{-1} and can be characterized as Si—O—Si(Al) bending vibrations[22].

Water in zeolites can be found bonded with each other (H_2O—H_2O) or with silanol framework. These water molecules may be found on the surface, in the cavities, channels or in small closed cages. Each of these possibilities should give different absorption bands for the OH of water, and this can be noticed[23] by the broad bands appearing between 3500–3100 cm^{-1}.

In general, the (O—H) bands of some zeolities have been reported at 3620–3600 and 3740–3715 cm^{-1} and are attributed to isolated bridge and silanol OH groups respectively[24-26].

IR-spectrum of unmodified zeolitic tuff samples: The sample DWZ bands at 3725, 3625 and 3565 cm^{-1} can be assigned due to ν(O—H) vibrations in different environments. Thus the band at 3725 cm^{-1} is assigned to terminal Si—OH, the band at 3625 cm^{-1} to bridge Si—OH—Si(Al) and the band at 3565 cm^{-1} is due to hydrogen bonding Si(Al)—OH.

The bonded water absorption broad bands are found at 3448 and 3260 cm^{-1}, which indicate the different types of bonding and location for the water molecules as shown in Fig. 1.

The bending vibration of H_2O is found at 1652 cm^{-1}. The strong asymmetric Si—O—Si(Al) stretching vibration at 1160 cm^{-1} are due to faujasite and chabasite and at 1020 cm^{-1} are due to phillipsite, faujasite and chabasite as shown in Fig. 2.

The symmetric Si—O—Si(Al) stretching vibrations appear at 780 cm^{-1} indicating the existence of chabasite, 730 cm^{-1} for faujasite, 672 cm^{-1} for phillpsite and 600 cm^{-1} for anorthite. The bending vibrations appear at 460 cm^{-1} for faujasite, at 455 cm^{-1} for chabasite and at 407 cm^{-1} for anorthite as shown in Fig. 3.

XRD measurements have revealed that calcite is present in the sample, so the band at 1420 cm^{-1} is due to asymmetric stretching vibration of the carbonate group. The reported value is at 1415 cm^{-1},[26] while bands appearing at 870 and 710 cm^{-1} are due to the bending vibrations of the same group. The reported value

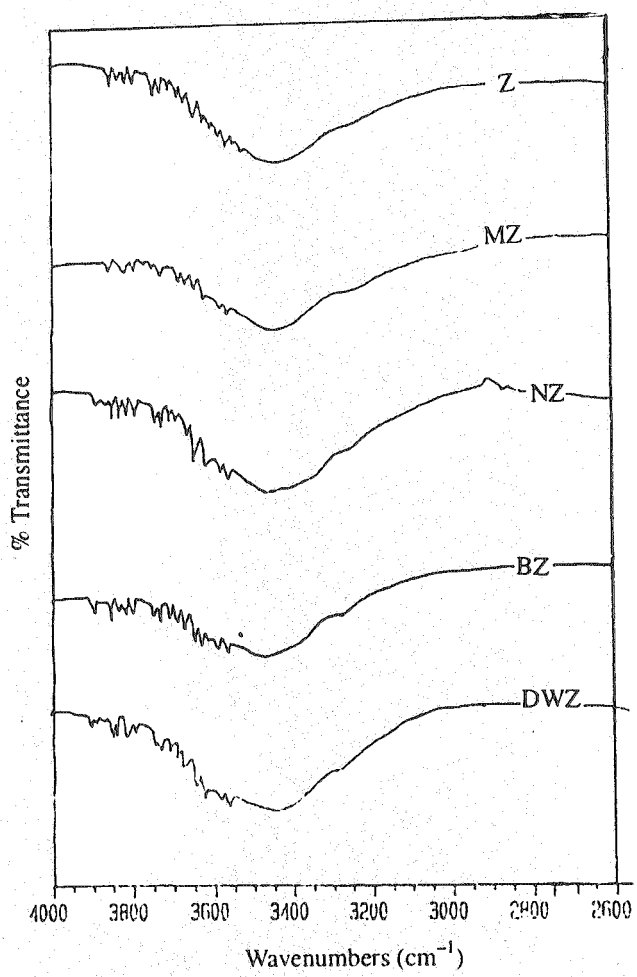

Fig. 1. Infrared spectrum of unmodified zeolitic tuff samples (4000–2600 cm^{-1}) region

is at 712 cm^{-1}.[28] The results of XRF and XRD indicate the existence of hematite in the mentioned samples. The absorption bands found at 464 cm^{-1} in Z sample and at 472 cm^{-1} in MZ sample in Fig. 3 confirm the existence of that in the samples. The reported value[28] for Fe_2O_3 is a strong absorption band at 470 cm^{-1}.

IR-spectrum of TiO_2 modified zeolitic samples: Fig. 4 illustrates the spectra of some modified and unmodified zeolitic tuff samples for the region lying between 4000–400 cm^{-1}. By a simple comparison of each pair of the modified and the unmodified samples, one can see that there is no significant change in the spectrum lying in the region between 4000–800 cm^{-1}.

Fig. 5 illustrates the IR spectra for the region lying between 800–400 cm^{-1} of the modified and unmodified pairs in comparison with the IR spectrum of TiO_2.

This will be used to illustrate change in DWZ spectrum when loaded with TiO_2 to produce TDWZ. Remarks will be made if any of the other samples shows any variations.

Concerning the spectrum of TMZ sample, the presence of weak absorption band at 472 cm^{-1} is due to the presence of hematite which is again in agreement with XRF and XRD results.

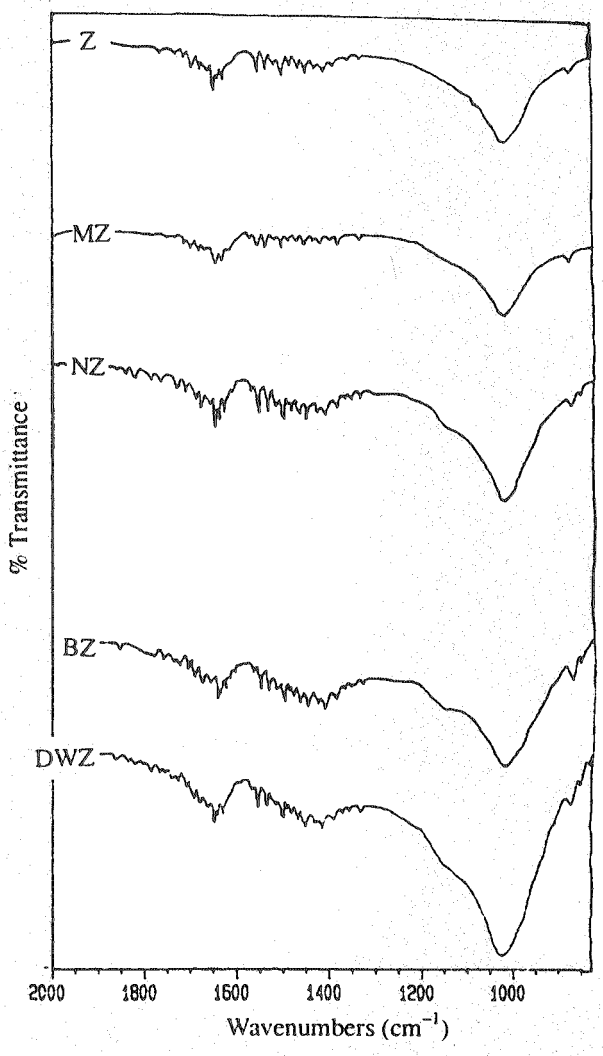

Fig. 2. Infrared spectrum of unmodified zeolitic tuff samples (2000–825 cm^{-1}) region

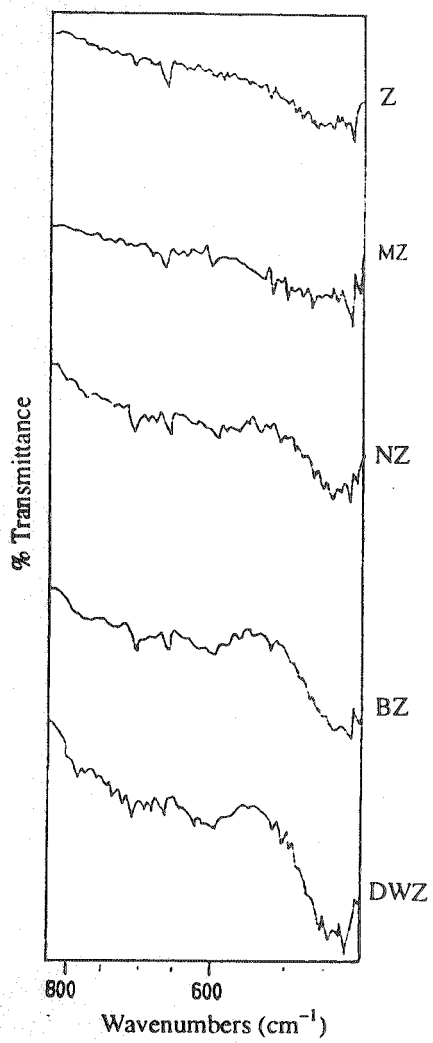

Fig. 3. Infrared spectrum of unmodified zeolitic tuff samples (825–400 cm^{-1}) region

Surface area estimation

The surface areas(A) and monolayer capacities (XM) for zeolitic tuff samples are shown in Table-7. The data given shows that while the removal of magnetic material from the raw zeolitic tuff, in sample NZ, considerably lowered the surface area by as much as 44%, the surface area of the iron-rich sample MZ shows almost no change. This may indicate that the iron in the raw tuff is present as the part of the zeolitic structure and its removal, as in sample NZ, results in the effective decrease in the net surface charge responsible for the adsorption of the methlylene-blue dye. This is because Fe^{3+} plays the same role as Al^{3+} in the zeolite matrix. Furthermore, the washing procedure to which NZ has been subjected to prepare samples DWZ and BZ has only slightly increased their surface areas by about 8% which may be attributed to the effective cleaning of the zeolite surface.

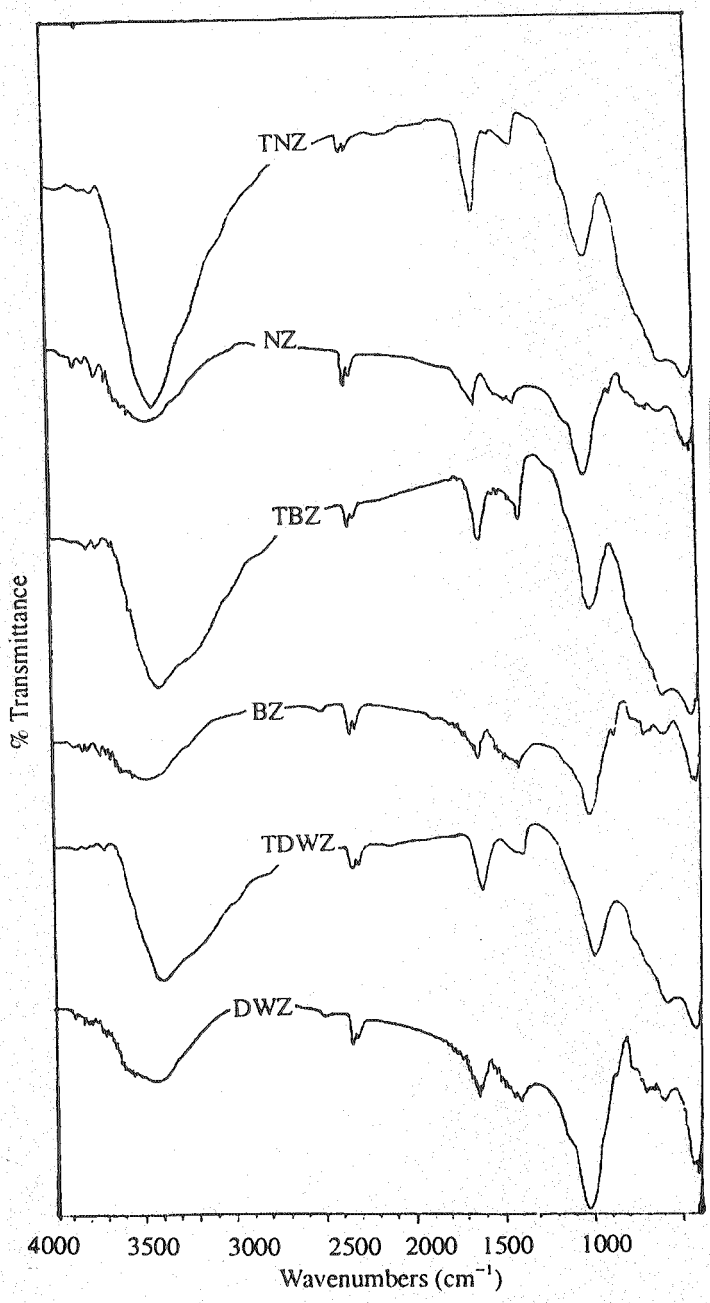

Fig. 4. Infrared spectra of DWZ, TDWZ, BZ, TBZ, NZ, and TNZ samples (4000–400 cm^{-1}) region

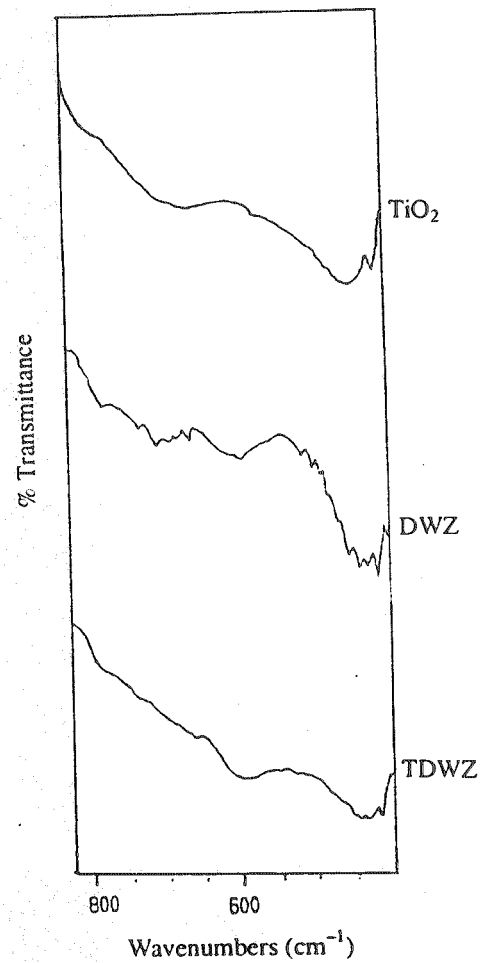

Fig. 5. Infrared-spectrum of DWZ, TDWZ, and prepared TiO_2 (800–400 cm^{-1}) region

As for the TiO_2 loading of the zeolitic tuff, Table-7 shows a decrease of 10–30% in the surface area. This interesting decrease may be attributed to the replacement of Al^{3+} and Fe^{3+} by Ti^{4+} thus effectively decreasing the negative surface charge responsible for the adsorption of the methylene-blue dye cation of the zeolite surface. This clearly illustrates the related decrease in Al_2O_3 content with the corresponding increase in TiO_2 in all samples.

The reaction of aqueous phenol

The detailed experimental data given in Table-8 summarize the result of the thermal oxidation of aqueous phenol with hydrogen peroxide in the presence of the different zeolitic tuff samples. Table-8 shows the per cent conversion for the thermal oxidation of phenol with H_2O_2. This per cent represents the ratio of the amount of phenol reacted to the initial amount of phenol used. The percentage conversion of phenol under the thermal conditions with the presence of the zeolitic tuff samples is calculated after 60 min from the beginning of the reaction, when the phenol concentration levels come up to be almost asymptotic to the time-axis.

TABLE-7
SURFACE AREA (A) AND MONOLAYER CAPACITY (Xm) OF ZEOLITIC TUFF SAMPLES

Sample	Monolayer capacity Xm ($\times 10^{-4}$)(mol/g)	Surface area A (m^2/g)
Z	1.790	129
TZ	1.570	113
MZ	1.840	133
TMZ	1.490	107
NZ	0.995	72
TNZ	8.290	60
DWZ	1.060	77
TDWZ	0.764	55
BZ	1.080	78
TBZ	0.835	60

Table-9 also gives the initial rate (v_0), initial rate constants and the conversion at 150 min for photochemical reaction of aqueous phenol, which are calculated from the initial slope when plotting concentration of phenol *vs.* time.

From Tables-8 one can notice that the presence of a catalyst in the reaction has speeded up the destruction of phenol remarkably. For example, when Z is used, the initial reaction rate has increased approximately 6 times.

It also noticed that the high iron containing zeolitic sample MZ has shown 3.3 times increase in the initial rate compared to Z sample, while the iron-poor sample NZ has shown a decrease of 3 times.

It can also be observed that all samples loaded with TiO_2 have shown remarkable increase in both the initial rates and percentage conversion in relation to the corresponding unmodified samples.

Fig. 6 shows the relation between the initial rates and the percentage conversion for the thermal oxidation at 20°C of aqueous phenol. Form this figure, it can be seen that samples which give high initial rate also give a high percentage conversion of phenol.

For the zeolitic tuff, again, the iron-rich samples MZ and TMZ have shown the highest initial rates and conversion in comparison with the other corresponding non-TiO_2 and TiO_2-loaded zeolitic tuff samples.

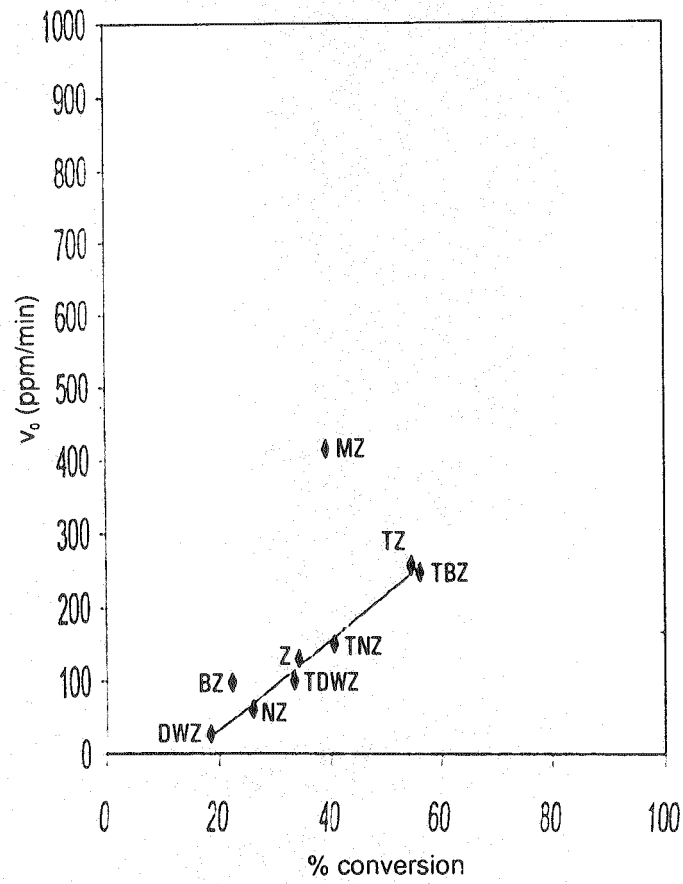

Fig. 6. Relation between % conversion and initial rales for thermal reaction of aqueous phenol

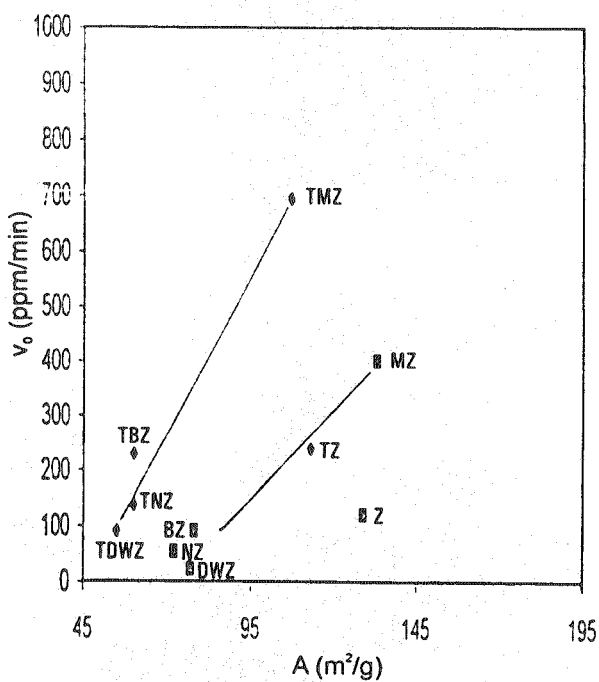

Fig. 7. Relation between surface areas of catalysts and initial rates for thermal reaction of aqueous phenol

TABLE-8
INITIAL RATES AND % CONVERSIONS AT 60 min FOR THE THERMAL REACTION OF AQUEOUS PHENOL WITH H_2O_2 OVER ZEOLITIC TUFFS

Sample	Initial rate (v_0)(ppm/min)	Conversion at 60 min (%)
No catalyst	20.00	7.22
TiO_2*	34.80	10.90
TiO_2**	72.00	18.34
Z	119.30	34.00
TZ	239.00	54.70
MZ	400.90	39.14
TMZ	694.14	67.34
NZ	53.00	25.78
TNZ	137.80	40.60
DWZ	21.80	18.30
TDWZ	90.00	33.20
BZ	90.10	22.06
TBZ	229.20	56.20

*Prepared TiO_2; **Merck TiO_2.

TABLE-9
INITIAL RATES, RATE CONSTANTS, INITIAL RATES CONSTANTS, AND THE % CONVERSION AT 150 MIN FOR THE PHOTOCHEMICAL REACTION OF AQUEOUS PHENOL IN THE ABSENCE OF H_2O_2 OVER ZEOLITIC TUFFS

Sample	Initial rate (v_0) (ppm/min)	Conversion at 150 min (%)	k# (min^{-1})	k_0# (min^{-1})
No catalyst	0.7	45	3.8 E-3	7.3 E-3
TiO_2*	6.0	70	7.8 E-3	4.3 E-3
TiO_2**	41.0	85	1.5 E-2	1.6 E-1
Z	5.6	75	7.8 E-3	6.6 E-2
TZ	12.0	82	1.0 E-2	7.4 E-2
MZ	6.0	93	1.8 E-2	5.4 E-2
TMZ	35.0	98	2.3 E-2	1.4 E-1
NZ	1.5	71	8.0 E-3	1.6 E-2
TNZ	5.5	73	7.4 E-3	6.5 E-2
DWZ	3.9	67	6.8 E-3	4.4 E-2
TDWZ	4.5	88	1.4 E-2	5.1 E-2
BZ	1.6	85	1.3 E-2	1.7 E-2
TBZ	14.0	93	1.7 E-2	9.2 E-2

*Prepared TiO_2. **Merck TiO_2. # k and k_0 were calculated assuming first order kinetics.

These high values can be attributed to the presence of iron. The role of iron can be understood in terms of the Fenton reaction, Fe^{3+}/H_2O_2 system[27]. The presence of Fe^{3+}, with H_2O_2 being added to the reaction, causes an increase in the producing of hydroxyl radicals (OH) which are active in the degradation of phenol. Moreover, despite the lack of enough energy to make TiO_2 to act as a semiconductor, all zeolitic tuff samples loaded with TiO_2 have shown an increase in the percentage conversion and initial rates for the thermal oxidation of aqueous phenol in relation to the other corresponding unmodified samples. TiO_2 loaded on the surfaces of different catalysts may have increased the efficiency of the active sites present on the surface.

Form Fig. 7 which shows the relation between surface area of catalyst and initial rate, one notices that an increase in the catalyst surface area for zeolitic samples is accompanied by an increase in the initial rate of the reaction.

Concerning the relation between the initial rate of the reaction and surface areas of the modified and unmodified pairs, one notices that although the modified samples have higher initial rate, they have lower surface area compared to their corresponding unmodified samples.

It is noticed that the decrease in the surface areas as determined by the methylene-blue method is due to the decrease in the charges on the solid surface caused by the replacement of Al^{3+} by Ti^{3+}, thus affecting the cationic adsorption capacity of the solid surface.

However, this does not seem to affect the active sites responsible for the oxidation of phenol by H_2O_2; both react through uncharged species, *viz.* hydroxyl radical initiated reactions. Consequently, the loading with TiO_2 seems to have increased the concentration of active sites leading to the marked increases in the initial reaction rates.

The point for sample TZ in comparison with the modified zeolitic tuff samples and sample Z in comparison with the other unmodified samples both fall outside the best lines drawn for other samples, but still show the same trend.

ACKNOWLEDGEMENT

The authors would like to thank the Natural Resources Authority for using their analytical facilities.

REFERENCES

1. I.M. Dwairi, Ph.D. Thesis, Hull University, U.K. (1987).
2. ———, Natural zeolites, The Third Geological Conference, Jordan (1988).
3. ———, *Dirasat,* **19B**, 23 (1992).
4. K. Ibrahim and A. Hall, *Eur. J. mineral.*, **7**, 1129 (1995).
5. K. Kato, M.J. Nageta, Y. Shakai, M. Shiba, M. Kojima and M. Onishi, *Iyo Kizai Kenkyusho HoKoKo,* **4**, 115 (1970).
6. S. Anderson, I. Grenth, E. Jansson and I. Naucler, *Ger. Offen.*, **2**, 512 (1975).
7. G.V. Tsitsishrili, T.G. Mikashrili, Kirov and L.D. Filizora, Natural Zeolites, Ellis-Horwood, Chichester (1992).
8. Z. Hagiwara and M. Vchida, in: L.B. Sand and F.A. Mumpton (Eds.), Natural Zeolites: Occurrence, Properties, Uses, Pergamon Press, Oxford, p. 463 (1978).

9. A.P. Mathews and C.A. Steve, *Environ. Prgr.*,**2**, 257 (1983).
10. R. Zeike and T. Pinnaravaia, *Clays Clay Minerals*, **36**, 403 (1988).
11. D. Chapman, Water Quality Assessments, Chapman & Hall, London (1992).
12. WHO Guidelines for Drinking-water Quality, Vol. 1: Recommendations, World Health Organization, Geneva (1993).
13. E. Salameh, Water Quality Degradation in Jordan, Natural Library, Jordan (1996).
14. M.A. Alwai, M.K. Fayyad and I. Issa, *Dirasat*, **17B**, 83 (1990).
15. V.C. Farmer, The Infrared Spectra of Minerals, 1st Edn., Mineralogical Society, London (1974).
16. P. Harben and M. Kazvart, Global Geology, 1st Edn., BPC Wheatons Ltd., London (1996).
17. K. Sabu, R.S. Kumar and M. Lilithambika, *Bull. Chem. Soc. (Jpn.)*, **66**, 3535 (1993).
18. R.I. Yousef, M.Sc. Thesis, University of Jordan, Jordan (1997).
19. I.M. Dwairi, *Dirasat*, **19B**, 7 (1992).
20. G. Blo, F. Doni and C. Bighi, *J. Chromatogr.*, **295**, 231 (1984).
21. R.I. Yousef, M. Tutunji, G. Derwish and S. Musleh, *J. Colloid. Interface Sci.*, **216**, 348 (1999).
22. V.C. Farmer, The Infrared Spectra of Minerals, 1st Edn., Mineralogical Society, London (1974).
23. G.V. Tsitsishrili, T.G. Andronikashrili, G.N. Kirov and L.D. Filizora, Natural Zeolites, Ellis-Horwood Limited, U.K. (1992).
24. J. Garcia, M. Gonzalez, J. Gaceres and J. Natorio, *Zeolites*, **12**, 664 (1992).
25. C.D. Diaz, S. Locatelli and E.E. Gonzo, *Zeolites*, **12**, 851 (1992).
26. V. Bhandarkar and S. Bhatia, *Zeolites*, **14**, 439 (1994).
27. G. Herzberg, Infrared and Raman Spectra of Polytomic Methods, D. Van Nostrand, New York (1945).
28. F.F. Bentley and S. Lee, Infrared Spectra and Characteristic Frequencies *ca.* 700–300 cm^{-1}, Interscience Publishers, New York (1968).

(*Received*: 8 July 2005 ; *Accepted*: 1 March 2006) AJC-4669